

Lidar Measurements Synchronized with Satellite Overflights Acquired at 14.64N 121.07E

¹Lorenzo de la Fuente, ²Susana Dorado, ³Nofel Lagrosas, ¹Columbo Enaje,
³John Holdsworth and ³Minella Alarcon

¹Manila Observatory, Quezon City, Philippines

²National Institute of Physics, University of the Philippines, Quezon City, Philippines

³Department of Physics, Ateneo de Manila University, Quezon City, Philippines

1. Introduction

Regular measurements using a Mie-scattering lidar have been obtained at a tropical location from July 1996 to December 1997. The measured backscatter intensity and linear depolarization ratio allow the calculation of extinction and backscatter coefficients. In addition to the verification of satellite observations these measurements characterize the local cloud and dust particulates and exhibit a seasonal variation.

2. Lidar system

The lidar site is located at 14.64 N 121.07 E within the Manila Observatory. A Q-switched Nd-YAG laser transmits an expanded, collimated and linearly-polarized 532 nanometer beam at 20 hertz. The backscatter is collected by a 28 centimeter diameter Schmidt-Cassegraine telescope in a biaxial vertical configuration, and directed through a collimating lens and a bandpass filter. From there the signal goes through a beamsplitter where parallel and orthogonal beam polarization components are directed to separate photomultiplier tubes (PMT). The analog voltage output from the two PMTs are digitized and averaged by a storage oscilloscope and saved using a microcomputer. Details of earlier configurations may be found in Alarcon et al. (1996).

3. Lidar observations

Figures 1 to 8 show time series plots of raw signal in volts for almost all measurement periods. Some measurement periods were not included because of insufficient duration, usually due to rain or equipment malfunction. The range gate most frequently used was 300 meters, but 600 and 1500 meter range gates were also used. Examples of high altitude measurements using a 1500 meter range gate are presented in De la Fuente et al. (1998). To make all time series plots intercomparable a voltage range of 0 to 0.2 volts was adopted for the Z-axis, an altitude range of 0 to 3000 meters for the Y-axis, and Local Standard Time (0800 LST is 0000 UTC) in decimal format for the X-axis. A summary of all modifications to the lidar equipment and measurement schedules that affected data acquisition is presented in Table 1. The schedule change on 14 January 1997 was implemented to accommodate a request from the Asian lidar network to make measurements that coincided with satellite overflights at the lidar site. Specific satellite platforms were not identified, but were probably polar orbiting satellites.

Table 1: Lidar system and schedule modifications

Date	Modification
05 December 1997	Q-switch failure
25 November 1997	data points changed 1000 points to 2500 points
21 November 1997	schedule changed 1930-2030 LST added
17 July 1997	operations resumed
22 May 1997	laser power supply failure
13 March 1997	configuration changed
04 February 1997	beamsplitter and depolarization PMT added configuration changed
14 January 1997	20.33 centimeter diameter telescope to 27.94 centimeter diameter telescope schedule changed
15 August 1996	0700-0900 and 1500-1700 LST to 0900-1000 and 1400-1500 LST regular schedule started 0700-0900 and 1500-1700 LST 20.33 centimeter diameter telescope single PMT installed 1000 data points

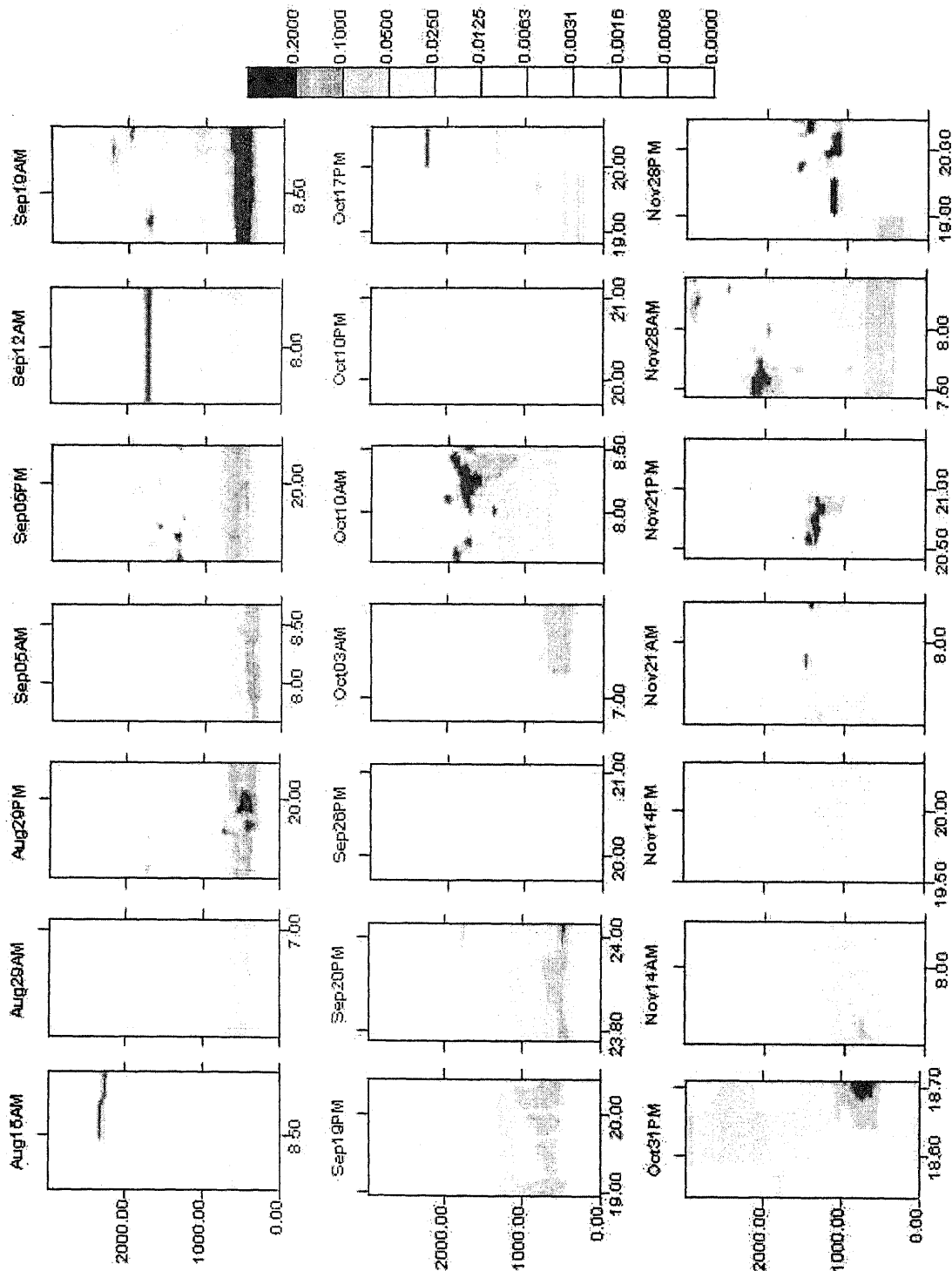


Figure 1: Signal Voltage from August to November 1996

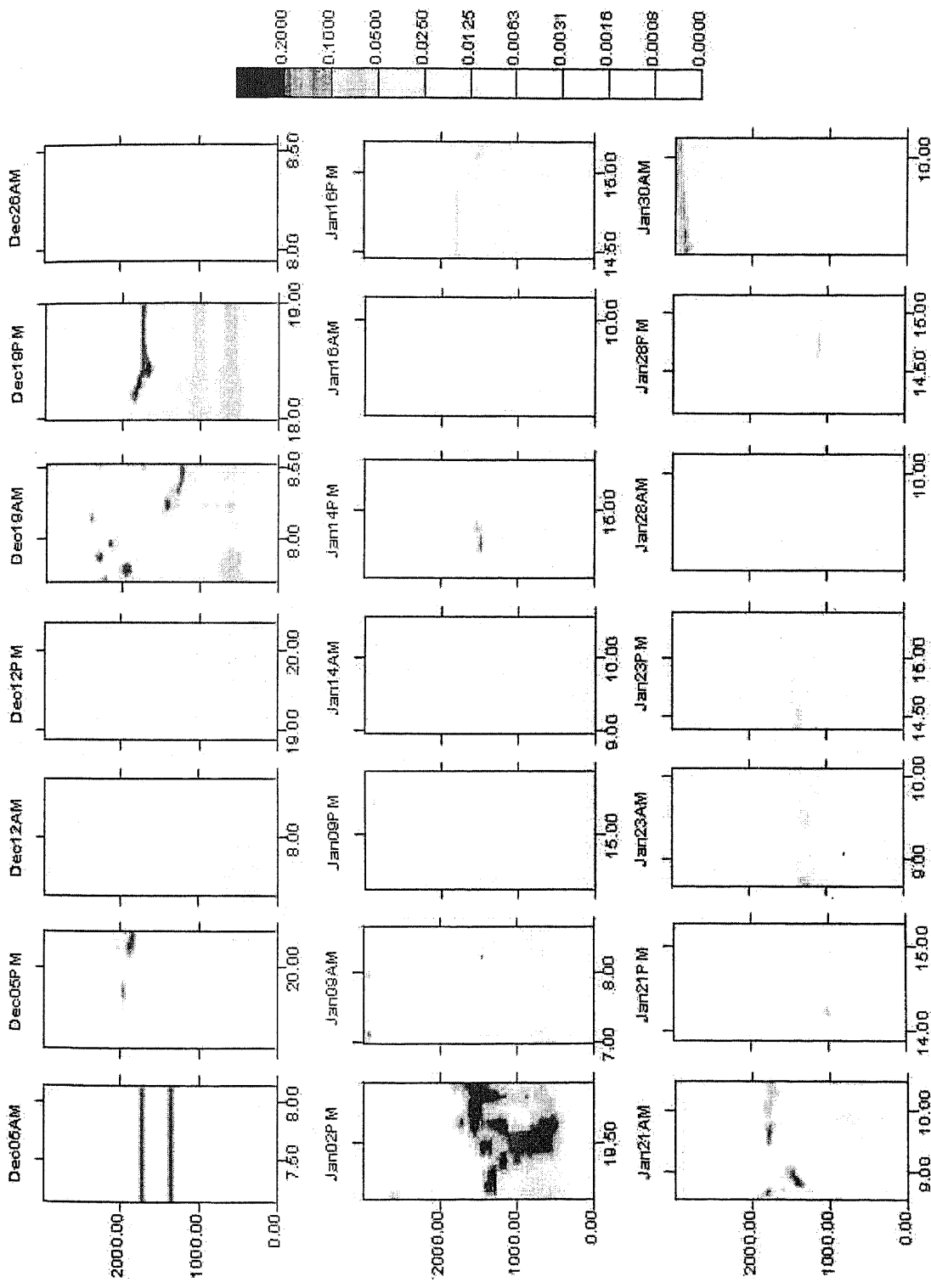


Figure 2: Signal Voltage from December 1996 to January 1997

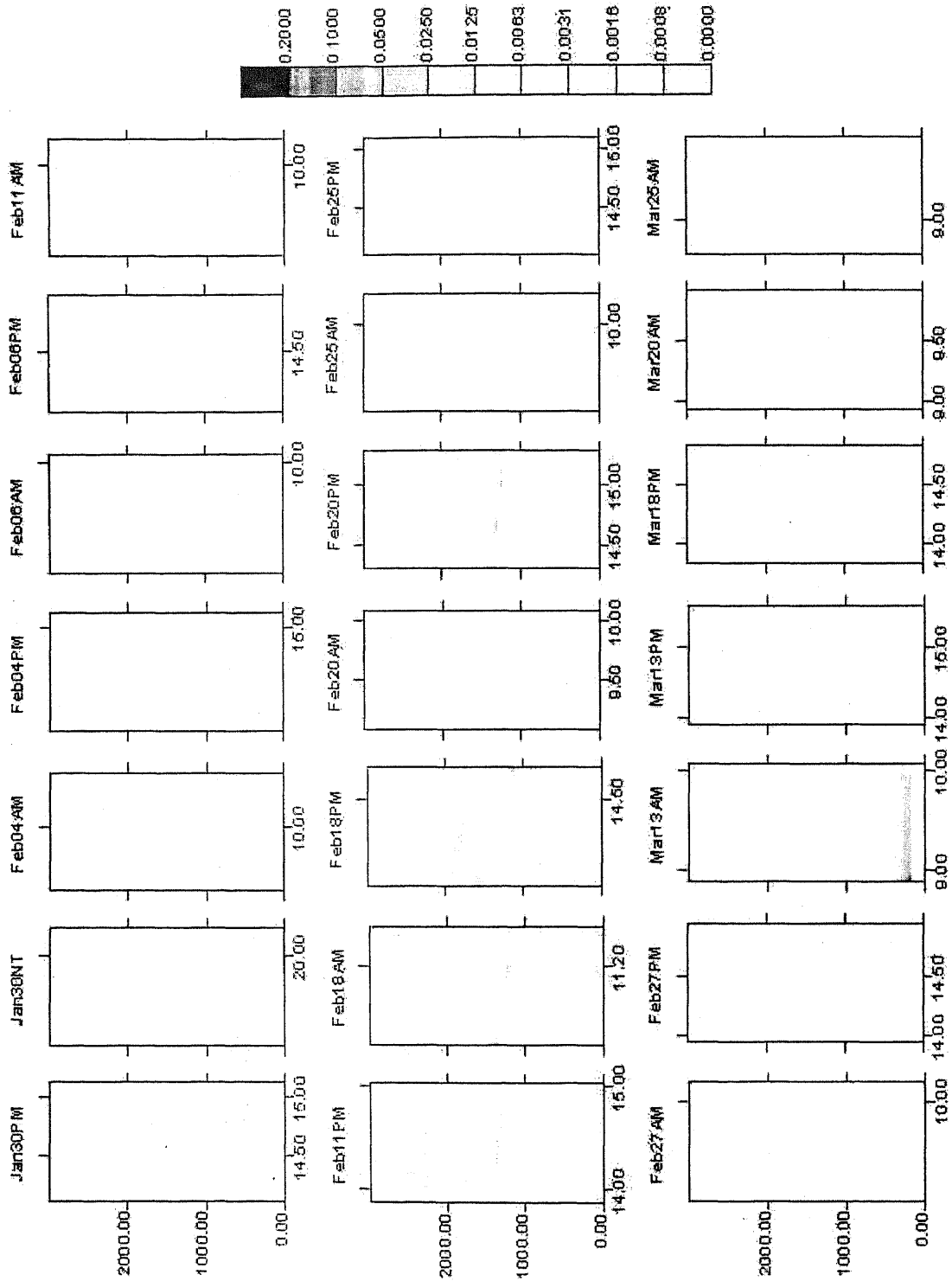


Figure 3: Signal Voltage from January to March 1997

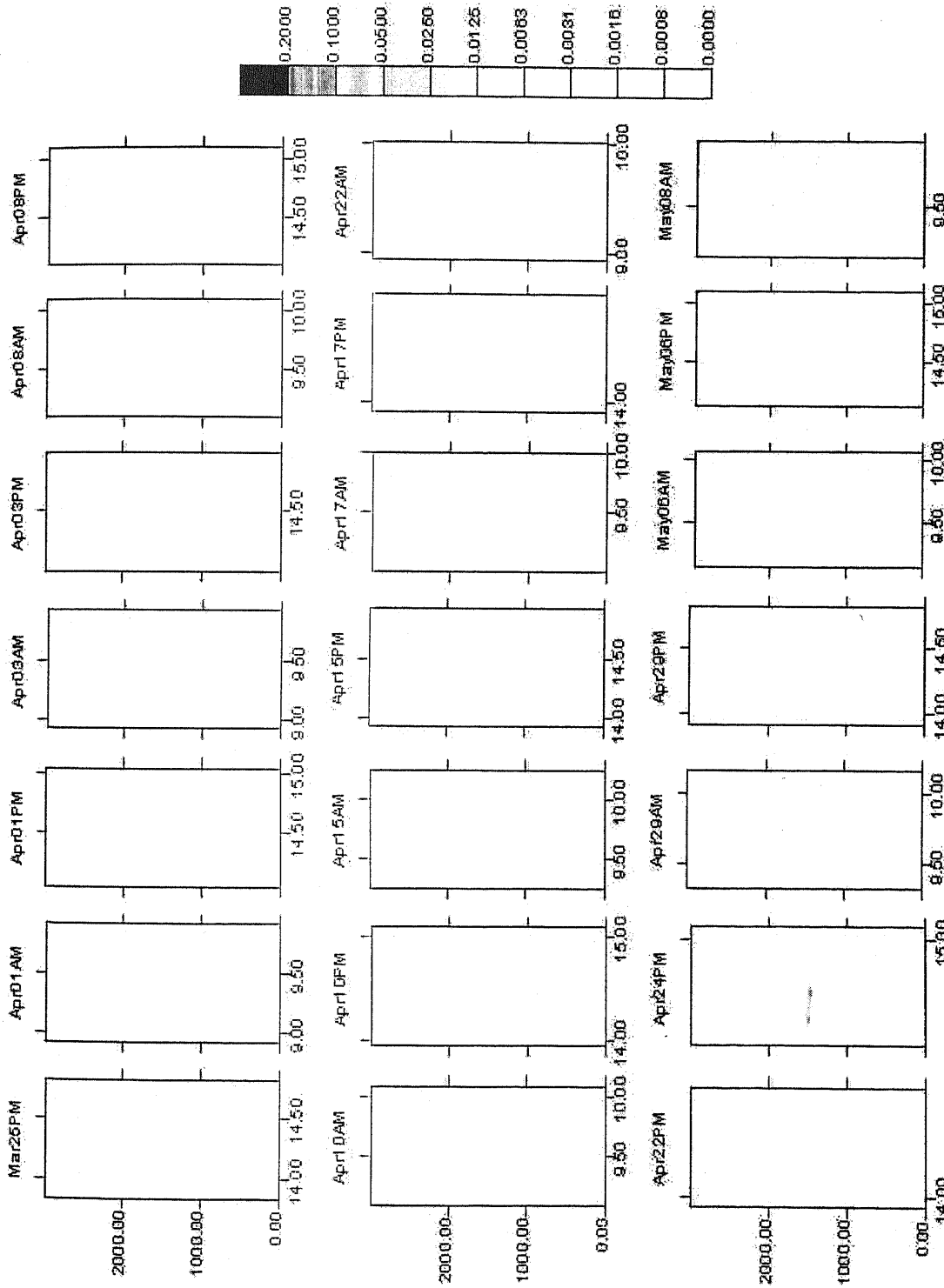


Figure 4: Signal Voltage from March to May 1997

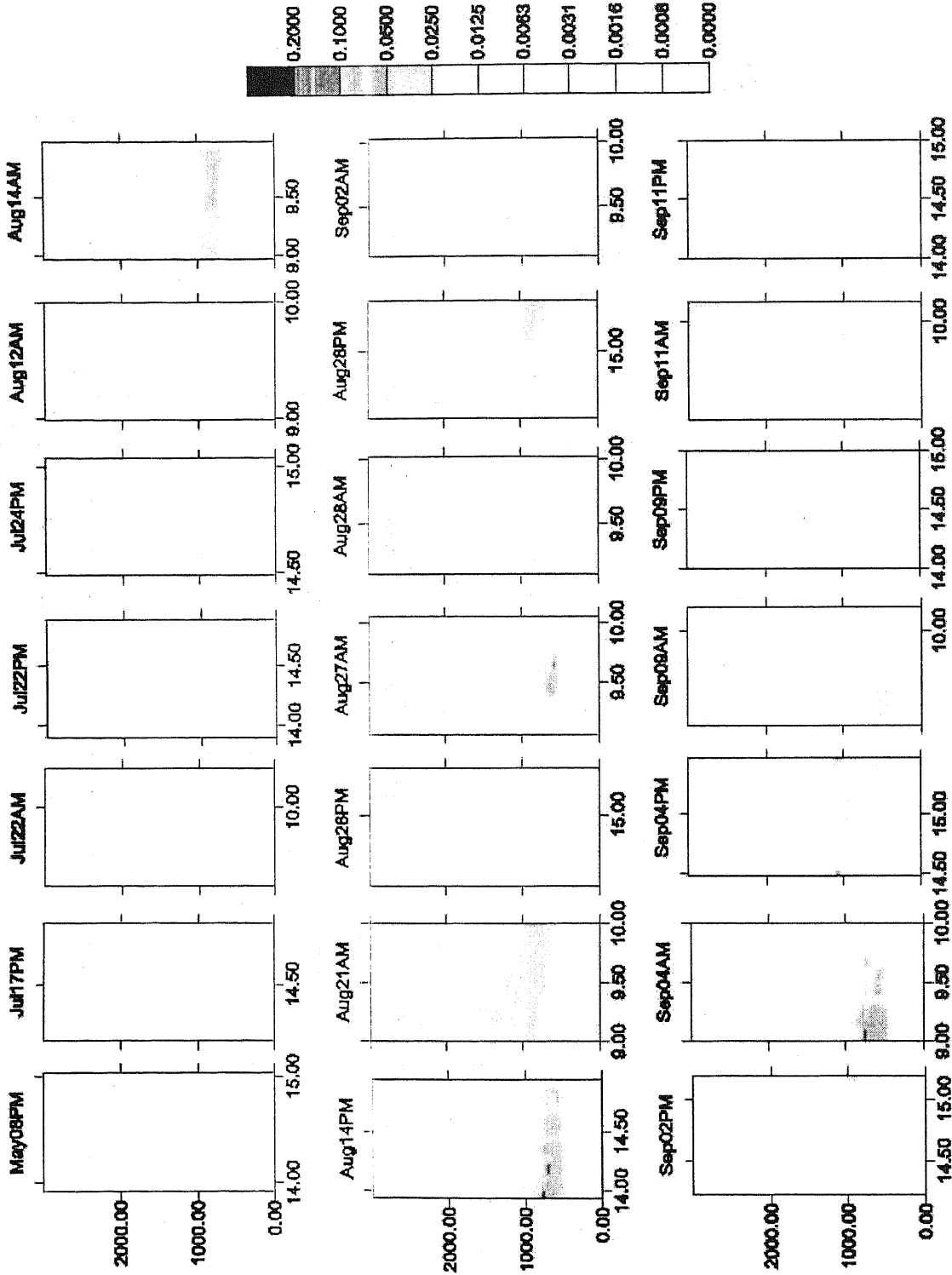


Figure 5: Signal Voltage from May to September 1997

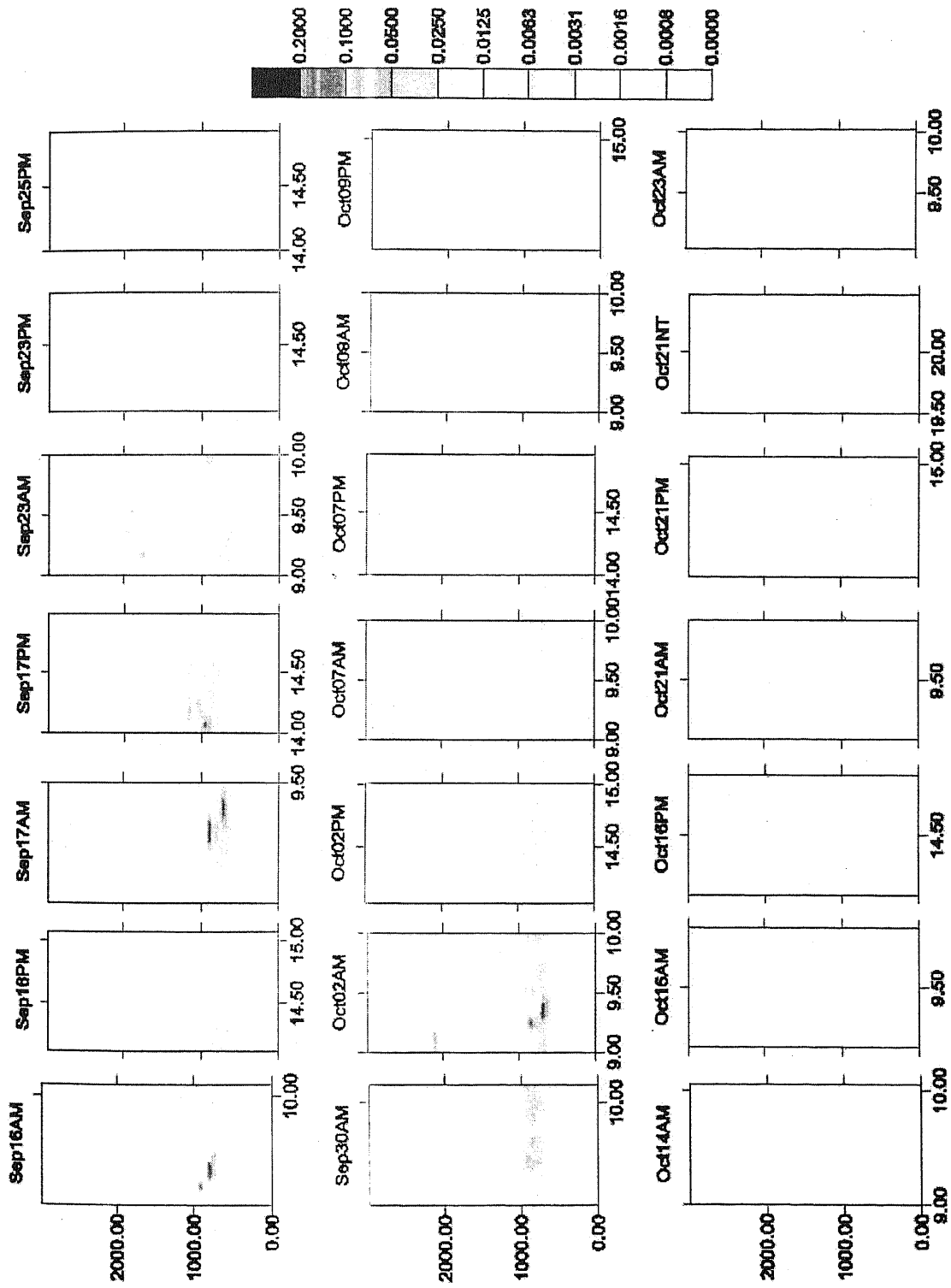


Figure 6: Signal Voltage from September to October 1997

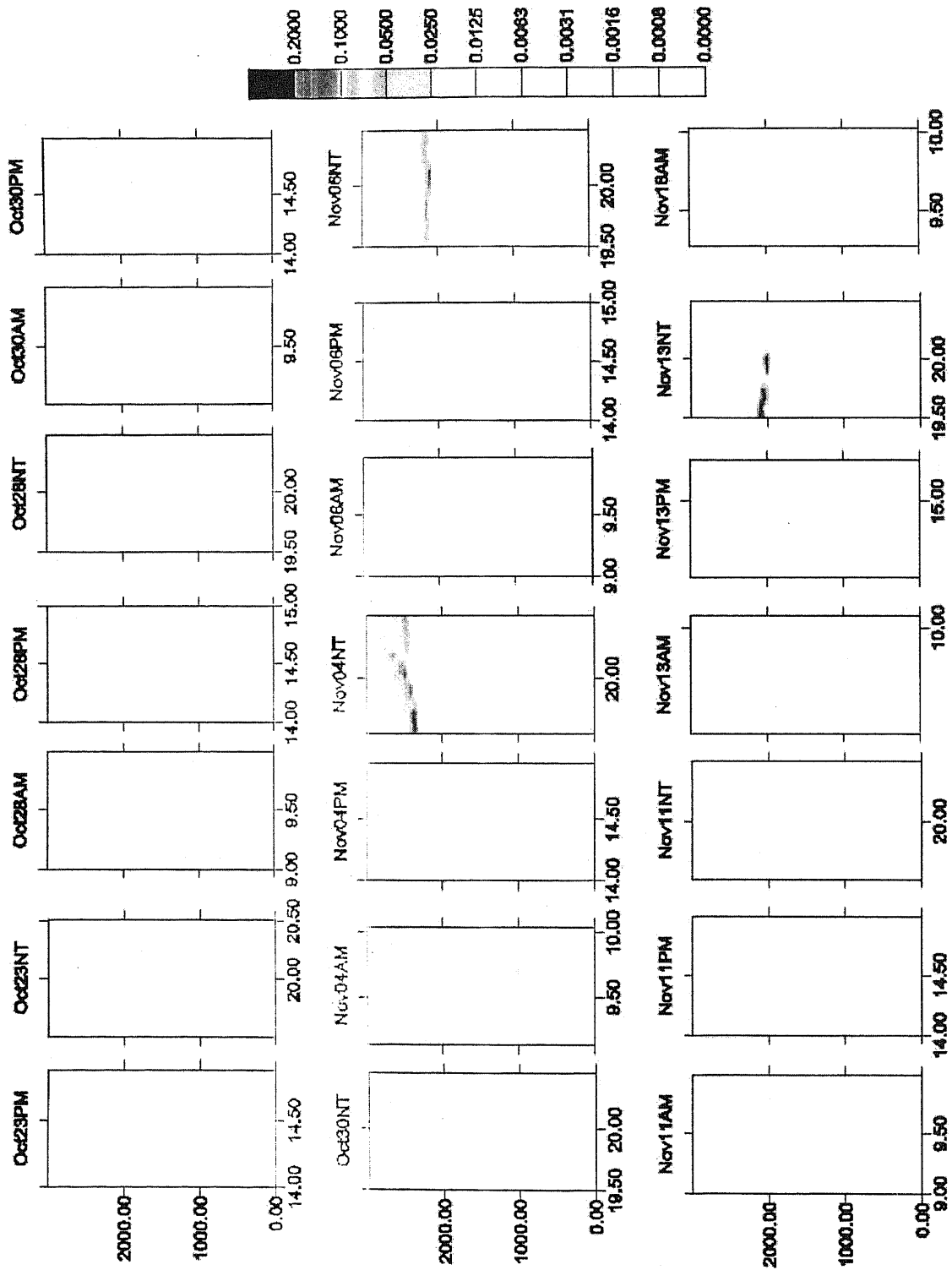


Figure 7: Signal Voltage from October to November 1997

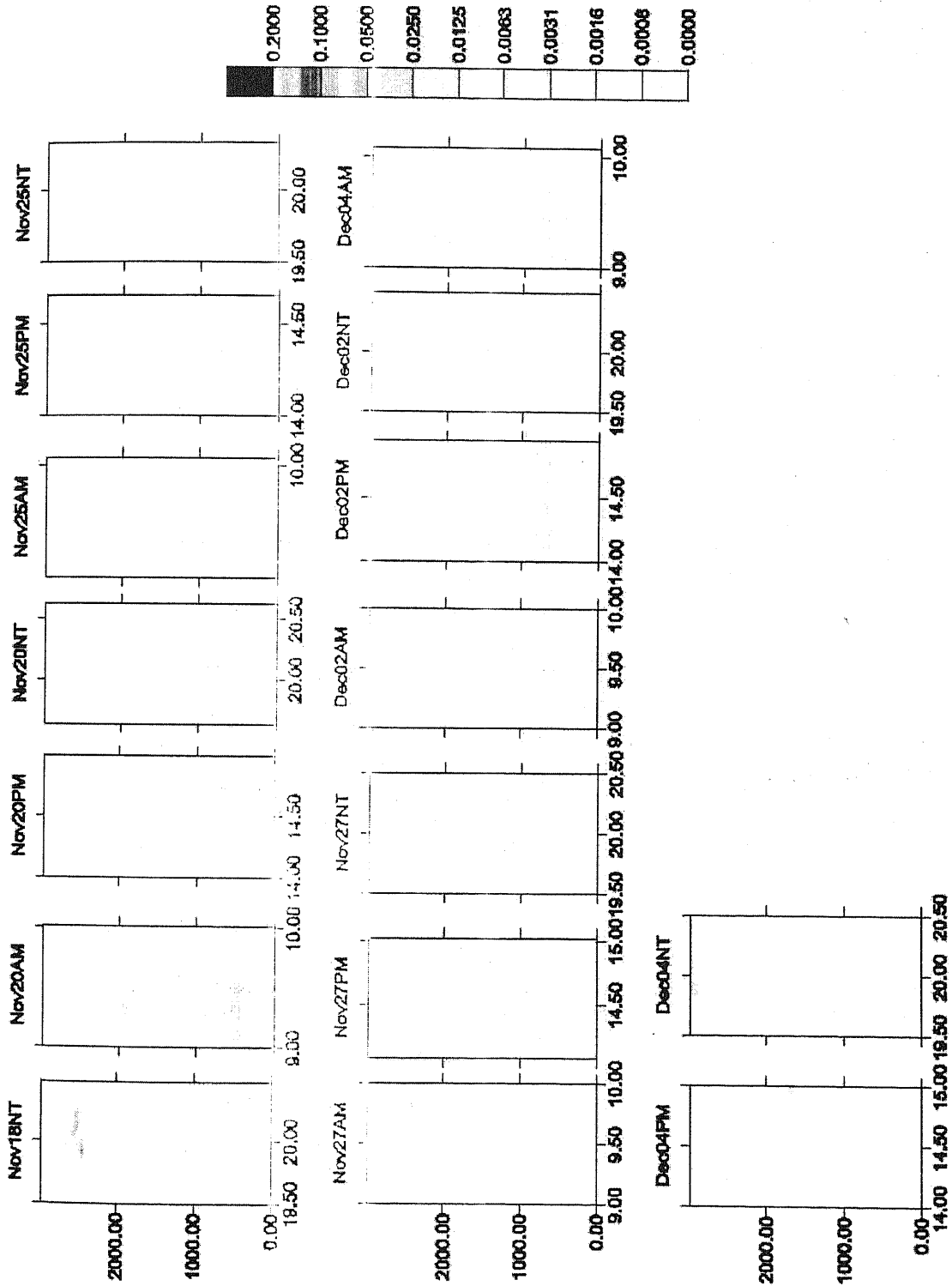


Figure 8: Signal Voltage from November to December 1997

4. Data inversion algorithms

Equipment and operational constraints introduce unavoidable variations in system parameters, which requires data to be constantly calibrated. Values for the system constant and backscatter to extinction ratio are then calibrated according to the method described by Russell et al. (1979). The following equations are expressions for particulate transmittance which may be combined to obtain an equation for the system constant:

$$R(r) = \frac{P(r)r^2}{K_{sys}T_R^2(r)T_P^2(r)\beta_R(r)} \quad (1)$$

$$T_P^2(r) = T_R(r)^{-\frac{3}{4\pi B}} \left[1 - \frac{2}{BK_{sys}} \int_0^r P(r')T(r')^{\frac{3}{4\pi B}-2} dr' \right] \quad (2)$$

Equation 1 may be solved for particulate transmittance. After setting it equal to equation 2 then solving for the system constant the equation becomes:

$$K_{sys} = \frac{P(r)r^2T_R(r)^{\frac{3}{4\pi B}}}{T_R^2(r)\beta_R(r)} + \frac{2}{B} \int_0^r P(r')T(r')^{\frac{3}{4\pi B}-2} dr' \quad (3)$$

The backscatter to extinction ratio is required in the computations for the system constant, and is determined using an equation derived from Fernald (1972):

$$B = \frac{1}{K_{sys}} \left[\int_0^r P(r')r^2T_R(r')^{\frac{3}{4\pi B}-2} dr' \right] \left[1 - T_P^2(r)T_R(r)^{\frac{3}{4\pi B}} \right]^{-1} \quad (4)$$

In order to solve for these parameters simultaneously an iterative process using equations 3 and 4 becomes necessary. The backscatter and extinction coefficients are then calculated following the method presented by Hughes et al. (1985). The laser-telescope overlap range varies slightly for each data collection period, but its altitude is generally about 500 meters. The extinction coefficient at the overlap range is calculated using an iterative method for the following transcendental equation:

$$k \ln \sigma(r_0) = S(r_0) + 2r_0\sigma(r_0) - \ln(K_{sys}B) \quad (5)$$

The extreme range varies with range gate setting, and is usually defaulted to the highest data point. The extinction coefficient at overlap range is used to calculate the extinction coefficient at extreme range using the following equation:

$$\sigma(r_f) = \left\{ \exp \left[\frac{S(r_f) + 2r_0\sigma(r_0) - \ln(K_{sys}B)}{k} \right] - \frac{2}{k} \int_{r_0}^{r_f} \exp \left[\frac{S(r') - S(r_f)}{k} \right] dr' \right\}^{-1} \quad (6)$$

Finally, the extinction coefficients between the overlap and extreme ranges are calculated using the following equation developed by Klett (1981):

$$\sigma(r) = \frac{\exp\left[\frac{S(r) - S(r_f)}{k}\right]}{\frac{1}{\sigma(r_f)} + \frac{2}{k} \int_{r_0}^{r_f} \exp\left[\frac{S(r') - S(r_f)}{k}\right] dr'} \quad (7)$$

The backscatter coefficients are calculated from extinction coefficients using a power law with the exponent set to unity.

5. Discussion

Seasonal variations in lidar backscatter are apparent from the progression of time series profiles, and appear to correspond to increased cloudiness during the rainy season (June-November) and decreased cloudiness during the dry season (December-May). Using data in figures 1 to 4, similar observations were made by Dorado et al. (1998). Rainy season cloudiness for 1997 appears to be less distinct than for 1996, which may be due to currently occurring regional El Niño effects. There also appears to be evidence of a gradual decrease in laser output power when comparing peak signals from mid 1996 and late 1997. At 0000 UTC on 05 August 1997 a specially arranged radiosonde launch occurred within 100 meters of the lidar site, and the data used for figures 9 and 10. Sample range-corrected lidar signals from the parallel and orthogonal PMTs are shown in figure 9, where high linear depolarization ratios indicate either multiple scattering or non-spherical scattering particles which may be dust. Figure 10 shows sample extinction and backscatter coefficient profiles calculated using lidar backscatter from the parallel PMT. The behavior of extinction and backscatter coefficients may be inferred from figures 1 to 8, since these optical parameters are directly proportional to signal voltage as shown in figure 10. Depolarization, extinction and backscatter measurements from Dorado et al. (1998) also exhibit seasonal and height-dependent variability which may be partly due to dust transport from the surface. The rest of the data is currently being analyzed, so time series plots of backscatter and extinction coefficients should be available soon.

Unsmoothed Data: 0012 UTC, 05 August 1997

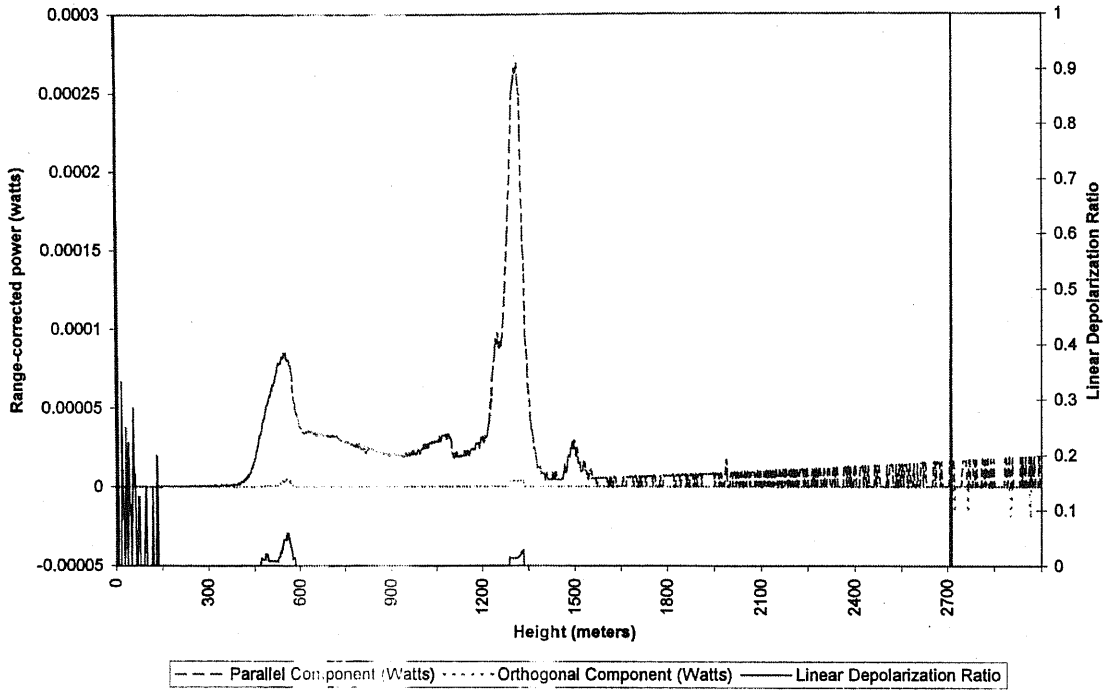


Figure 9: Range-corrected power and depolarization ratio for 0012 UTC, 05 August 1997

Optical Parameters: 0012 UTC, 05 August 1997

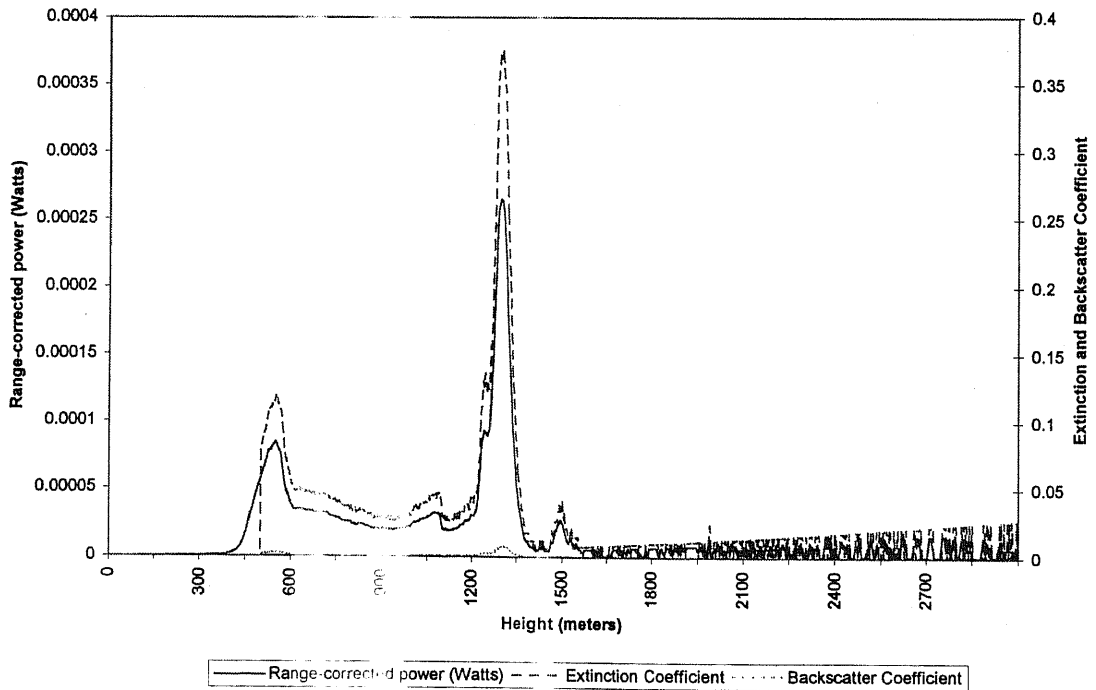


Figure 10: Extinction and Backscatter coefficients for 0012 UTC, 05 August 1997

References

- Alarcon, M., S. Dorado, J. Holdsworth, B. Sychingiok, and D. McNamara. 1996: Mie lidar measurements in Metro Manila (14.64N, 121.07E). *Extended Abstracts, 18th Int. Laser Radar Conf.*, Berlin, International Coordination Group on Laser Atmospheric Studies, 167
- De la Fuente, L., M. Alarcon and S. Dorado. 1998: *Tropical Cloud Optical Phenomena and Pioneering Lidar Observations at the Manila Observatory*. Bull. Of the Amer. Meteor. Soc. 79, 5-7
- Dorado, S., N. Lagrosas, L. de la Fuente, J. Holdsworth and M. Alarcon. 1998: *Mie Backscatter Intensity and Depolarization Measurements of Tropical Clouds at 14.64N 121.07E in the Philippines*. Submitted to J. of Atmos. Sci.
- Fernald, F., B. Herman, and J. Reagan. 1972: *Determination of Aerosol Height Distribution by Lidar*. J. of Appl. Meteor. 11, 482-489
- Hughes, H., J. Ferguson and D. Stephens. 1985: *Sensitivity of a Lidar Inversion Algorithm to Parameters relating Atmospheric Backscatter and Extinction*. Appl. Opt. 24, 1609-1613
- Klett, J. 1981: *Stable Analytical Inversion Solution for Processing Lidar Returns*. Appl. Opt. 20, 211-220
- Liou, K. 1980: *An Introduction to Atmospheric Radiation*. International Geophysics Series v.26. Academic Press. 392 pp.
- Russell, P., I. Swissler and M. McCormick. 1979: *Methodology for Error Analysis and Simulation of Lidar Aerosol Measurements*. Appl. Opt. 18, 3738-3799